ELSEVIER

Biomaterials 22 (2001) 1971–1985

Biomaterials

www.elsevier.com/locate/biomaterials

Hydrophilic hybrid IPNs of segmented polyurethanes and copolymers of vinylpyrrolidone for applications in medicine

Gustavo A. Abraham[a,c], Alvaro A.A. de Queiroz[b], Julio San Román[a,*]

[a]*Instituto de Ciencia y Tecnología de Polímeros, CSIC, Juan de la Cierva 3, 28006 Madrid, Spain*
[b]*Departamento de Física e Química, Instituto de Ciencias — Escola Federal de Engenharia de Itajubá, Av. BPS 1303, 37500-000 Itajubá-MG, Brazil*
[c]*Instituto de Investigaciones en Ciencia y Tecnología de Materiales (INTEMA) (UNMdP-CONICET), Av. J.B. Justo 4302, 7600 Mar del Plata, Argentina*

Received 7 January 2000; accepted 6 November 2000

Abstract

The preparation and biocompatibility properties of thermoplastic apparent interpenetrating polymer networks (T-IPNs) of a segmented polyurethaneurea, Biospan™ (BS), and vinylpyrrolidone–dimethylacrylamide (VP–DMAm) copolymers, are described. The biological interaction between the obtained materials and blood was studied by in vitro methods. The addition of the VP–DMAm copolymers to form T-IPNs with BS substantially increased the equilibrium water uptake and water diffusion coefficients. Investigation of the proteins adsorption, platelet adhesion, thrombus formation and factor XII activation is presented. Investigations of the proteins adsorption of the BS/VP–DMAm T-IPNs surfaces show that the segmented polyurethane (BS) containing VP–DMAm copolymers with higher VP content adsorb more albumin than fibrinogen and γ-globulin. The platelets adhesion, thrombus formation and factor XII activation are effectively suppressed with respect to the segmented polyurethane when VP–DMAm copolymers with high VP contents are incorporated into BS as T-IPNs. © 2001 Published by Elsevier Science Ltd.

Keywords: Segmented polyurethanes; Thermoplastic IPNs; VP–DMAm; Blood compatibility; Proteins adsorption

1. Introduction

Modern medical devices are made from a wide range of materials including polymers, metals and ceramics. Due to the higher surface free energy of the metallic or ceramic medical devices, their surfaces in general are coated with biologically inert polymers. Thus, polymers with good film-forming properties provide coatings with much more biocompatibility than the original surfaces and they have been extensively used in implantable devices such as extracorporeal circuit components [1], thoracic drain catheters [2], vascular grafts [3], dialysis membranes [4] and percutaneous transluminal coronary angioplasty [5].

Most of the present-day companies provide polymeric coatings with biological activity or coatings to promote host-cell overgrowth as different means of producing blood-compatible surfaces for devices that will be used in clinical procedures [6].

Segmented polyurethanes (SPUs) have been considered for potential use in biomedical devices because of their good mechanical properties, their resistence to biodegradation as well as their biocompatibility for long-term implant applications [7–12].

It is very well known that SPUs are multiblock polymers composed of soft and hard segments which constitute a microphase-separated structure [13,14]. The soft-segment phase is, in general, the continuous phase and the hard segments act as both reinforcement of the soft matrix and physical crosslinks. This characteristic confers on SPUs unique elastomeric properties and makes them a choice for a wide variety of biomedical devices in which blood-contacting polymer is of a crucial importance.

The treatment of end-stage chronic heart failure (CHF) is just an example of the importance of the SPUs applications in the cardiovascular field and this particular heart disease remains a major challenge for physicians to overcome [15].

* Corresponding author.
E-mail address: ictsr04@ictp.csic.es (J.S. Román).

0142-9612/01/$ - see front matter
PII: S0142-9612(00)00381-1

The segmented polyurethane, Biospan™ (BS), displaying blood compatibility and resilience has been the material of choice for a wide variety of thin-film applications. BS, is supplied by The Polymer Technology Group (USA) as a 25% (wt/wt) solution in dimethylacetamide.

Bladders and coatings for long-term left ventricular assist blood pumps, intra-aorta ballon pumps as well as blood bags and compensatory chambers represent prominent applications of segmented polyurethane Biospan™ as a blood-contacting polymer [16,17].

Although a large number of publications have appeared describing the applications of segmented polyurethanes for implantable devices, microscopic thrombi and evidence of microemboli have been observed in some cases [18]. This gives limitations for long-time applications.

It is known that a number of polymer surface parameters are responsible for the antithrombogenic property of the synthetic polymer materials such as surface composition and morphology, hydrophilic/hydrophobic character, surface free energy and surface charge [19–24]. An increasing number of publications have been devoted to the preparation of thermoplastic apparent interpenetrating polymer networks (T-IPNs) as a means of tailoring the bulk and the surface properties of polymeric materials for blood-contacting devices [25,26].

T-IPNs are based on combinations of physical crosslinked polymers or physical crosslinked and linear polymers, in other words T-IPNs are hybrids between polymer blends and IPNs that involve physical crosslinks rather than chemical cross-links [27,28].

A unique feature of these systems is that the surface composition as well as structure and consequently the surface properties of the material are often different from that of the bulk due to a surface enrichment of the component that will minimise the total surface energy of the system [26].

It has been pointed out that amphiphilic copolymers provide an excellent way for the preparation of macromolecular systems with a specific microdomain structure that affects the platelet adhesion and activation [29,30]. Thus, the biochemical properties of these copolymers such as interactions with proteins and adsorption of blood cells will depend upon the monomers or comonomers of which they are made.

Biospan™ is a segmented polyurethane composed of a soft segment (PTMO, polytetramethylene oxide, $M_w = 2000$ g/mol) and a hard segment (MDI, 4,4′-diphenylmethane diisocyanate extended with a mixture of ethylene diamine–1,3-cyclohexanediamine).

Poly(*N*-vinyl-2-pyrrolidone) (PVP) and poly(*N*,*N*′-dimethylacrylamide) (PDMAm) are one of the most frequently investigated classes of materials for use in medicine and in other applications interfacing with biological systems [31–34].

The principal reasons for successful PVP and PDMAm applications are their excellent biocompatibility with living tissues and extremely low cytotoxicity [35,36]. PVP and PDMAm are amorphous polymers with glass transition temperatures of 177 and 84°C, respectively. These polymers have been subjected to various patents for preparing hydrophilic polyurethane coatings [37–39].

Composed of a lactam and amide groups, vinylpyrrolidone–dimethylacrylamide (VP–DMAm) copolymers should be able to interact with aromatic aminoacid residues of proteins via charge-transfer interactions without conformational change of the biological compound [40].

Thus, the polymer systems chosen in our study are composed of two components with thermodynamic compatibility: BS and hydrophilic VP–DMAm copolymers. The molecular structures of BS and VP–DMAm are shown in Fig. 1.

The aim of this study was to compare the blood compatibility of BS/VP–DMAm T-IPNs relative to BS. The hydrophilic materials obtained were compared to hydrophobic BS with respect to both albumin and fibrinogen adsorption as well as platelet adhesion and activation.

2. Experimental

2.1. Materials

Biospan™, a segmented poly(ether urethane urea) linear block copolymer of 4,4′-diphenylmethane diisocyanate (MDI) extended with a mixture of ethylene diamine, 1,3-cyclohexanediamine and PTMO 75% wt/wt was purchased from The Polymer Technology Group, USA. This polymer contains as additive a linear copolymer of diisopropylaminoethylmethacrylate and decylmethacrylate 5% wt/wt based on dry polymer. Biospan™ was provided in *N*,*N*-dimethylacetamide concentration consisting of 25% wt/wt and was diluted to 12.5% wt/wt to reduce the viscosity. *N*,*N*-dimethylacetamide (DMAc, Scharlau) was used without further purification.

2.2. Copolymers synthesis

Random copolymers of *N*-vinyl-2-pyrrolidone (VP) and *N*,*N*′-dimethylacrylamide (DMAm) were prepared and characterised according to the method described in our previous publication [41]. Briefly, copolymerisation reactions between VP and DMAm were carried out under vacuum in ethanol as the solvent using azobis(isobutyronitrile) (AIBN) (1.5×10^{-2} mol/l) as initiator, at 50°C. The resultant copolymers were precipitated from solution with diethyl ether and subsequently redissolved (in ethanol) and reprecipitated to minimise the presence of residual unreacted monomer and then, dried under vacuum to constant weight. The ^{1}H-NMR and ^{13}C-

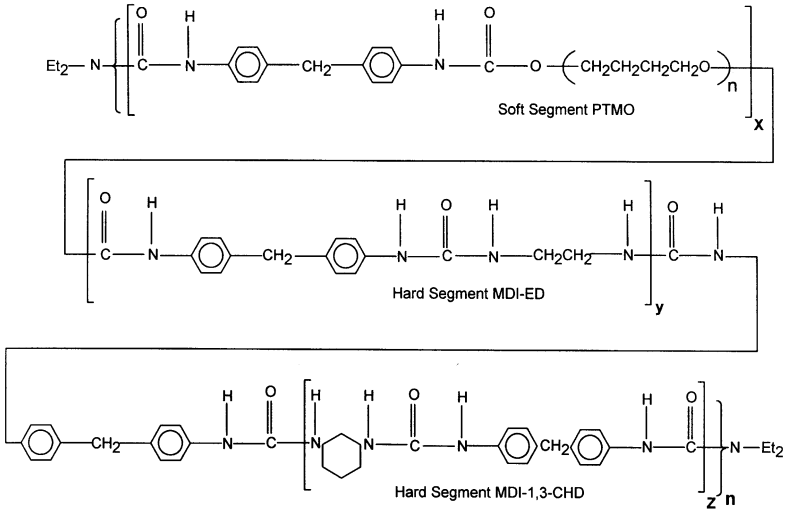

Idealized structure of segmented polyurethane (BS)

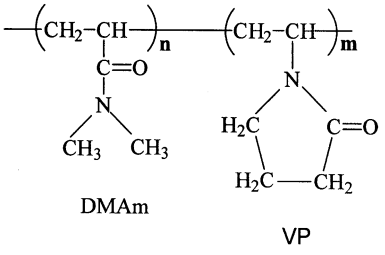

DMAm-VP copolymer structure

Fig. 1. Molecular structures of BS and the copolymer used in this work.

NMR spectroscopy were used to determine the precise average molar composition and purity of the synthesised copolymers.

2.3. T-IPNs preparation

The T-IPNs were formulated to contain 30% (w/w) of the poly(VP-co-DMAm) in relation to the segmented polyurethane (BS). Thus, an amount of the BS solution (12.5% wt/wt) in DMAc was mixed with 2 ml of the VP–DMAm copolymers previously dissolved in DMAc. The weight percentages of the VP or DMAm on the added copolymers are shown in Table 1. The sample nomenclature used in Table 1 and throughout this work indicates the type and corresponding weight percentage of copolymers in prepared T-IPNs. Thus, sample VP8BS refers to a T-IPN composed of a VP–DMAm copolymer of compositions 8 wt% VP and 92 wt% DMAm. After stirring at 25°C for 2 h, films were prepared by casting from the DMAc solutions onto Teflon® plates. The films were cast in one layer with evaporation of the solvent (24 h at 60°C). Final drying was done in a vacuum oven (3 mmHg) at 60°C for 48 h. The incorporation of VP–DMAm copolymers in the Biospan™ solution did not cause precipitation of the segmented polyurethane. The solutions remained clear, indicating homogeneous mixing within the segmented polyurethane solution. All samples were transparent in the dehydrated state.

Table 1
VP weight percentage of T-IPNs components in the dehydrated state

Sample	W_{VP} (wt%)	W_{DMAm} (wt%)
BS	0	0
VP8BS	8	92
VP29BS	29.3	70.7
VP63BS	62.7	37.3
VP100BS	100	0

2.4. Characterisation of T-IPNs systems

2.4.1. Attenuated total internal reflectance-FTIR (ATR-FTIR)

Infrared analyses were performed using a Nicolet 520 infrared spectrometer equipped with an ATR accessory (Spectra-Tech Inc., Model 300). The spectra were recorded at an incident angle of 45° using a Ge crystal, giving an analysis depth of 1–2 μm.

2.4.2. Fluorescence spectroscopy

A Perkin Elmer LS 50B luminescence spectrophotometer was used for recording the emission and excitation spectra of each BS/VP–DMAm T-IPNs film. The spectrum of each film was obtained at room temperature in air using 2 mm slit widths. Excitation spectra were subsequently normalised with respect to the lamp intensity fluctuations by dividing each spectrum by that obtained with a rhodamine-B standard solution. All the emission spectra were recorded in the range 270–400 nm at an excitation wavelength of 230 nm and with the slit at $E_x/E_m = 12/5$. The sample film was analysed at an angle of 45° to the beam of excitation light in order to prevent any scattered light from entering the emission monochromator.

2.4.3. Phase contrast microscopy

A polarised light microscope Nikon Eclipse E400 was used to determine the morphological textures of the obtained BS and BS/VP–DMAm T-IPNs films.

2.4.4. Differential scanning calorimetry (DSC)

Differential scanning calorimetry was performed on the copolymer samples by using a Perkin-Elmer DSC-7. Nitrogen was used to purge the DSC cell at a flow rate of 50 ml/min. Sample weights ranging from 5 to 15 mg, were hermetically sealed in aluminium pans. Samples were heated at a rate of 10°C/min.

The glass transition temperatures (T_g) of the Biospan™/VP-co-DMAm polymer systems were determined at the onset of the transition of DSC traces, respectively.

2.4.5. Contact angle

The sessile drop technique was employed to measure the contact angle of liquids with known surface tension on T-IPNs films. The liquids in this study are water ($\gamma_L = 72.8\,mJ/m^2$) and methylene iodide ($\gamma_L = 51.0\,mJ/m^2$) [42]. The geometric mean method was used to deduce the surface free energy of the T-IPNs films from the contact angles of two different liquids, water and methylene iodide [43]. The spatial size probed (in the plane of the surface) is 1–2 mm in diameter.

2.4.6. Water sorption and diffusion

The water sorption and diffusion measurements were obtained after known weights of the dry BS and BS/VP–DMAm T-IPNs films were immersed in phosphate-buffered saline (0.1 M NaCl, 0.086 M KH_2PO_4, 0.041 M Na_2HPO_4, pH 7.4) (PBS) at 37°C until equilibrium was reached. Then the films were removed, blotted quickly with absorbent paper to eliminate the water attached on its surface and weighed. The swelling behaviour of the films was calculated from the following relation:

$$\text{Swelling}\,(\%) = (W_t - W_0/W_0) \times 100,$$

where W_t is the weight of swollen film at time t and W_0 is the initial mass of the film.

2.5. Biological properties of BS and BS/VP–DMAm T-IPNs

2.5.1. Protein adsorption from plasma

Quantitative adsorption of albumin (Alb), fibrinogen (Fbg) and immunoglobulin G (IgG) to BS/VP–DMAm T-IPNs was determined by enzyme immuno assay (EISA) technique according to the method of Breemhaar and Van Dame [44,45]. The human proteins Alb, IgG, Fbg and citrated human plasma were purchased from the Clinical Analyses Laboratory of the Camilo Castelo Branco University/Faculty of Pharmaceutical Sciences (CAL/UCCB, SP/Brazil). Rabbit serum samples directed against Alb, IgG and Fbg (first antibodies) were obtained from CAL/UCCB. Before use the serum samples were diluted 100 times in phosphate-buffered saline (0.1 M NaCl, 0.086 M KH_2PO_4, 0.041 M Na_2HPO_4, pH 7.4) (PBS) containing 1% bovine serum albumin (PBS-BSA). BS and BS/VP–DMAm T-IPNs films of 0.9 cm^2 surface area were put in contact with 500 μl of PBS at 37°C. Binding of serum proteins on the BS and BS/VP–DMAm T-IPNs was determined after 1 h of incubation with 500 μl of the first antibody solution (1% v/v) at 37°C. After 1 h of incubation at 37°C, the films were rinsed 3 times with 150 μl of PBS containing Tween 20 (0.005% w/v) (PBS/Tw). Negative controls were obtained with the addition of PBS/Tw solution to the control plates. Then 500 μl of a solution of the horse-radish peroxidase-labelled second antibody (Biochemical, conjugate 200 times diluted) was added. All first and second antibodies were polyclonal. After rinsing 3 times with 150 μl PBS-Tw, 100 μl of buffer solution containing the hydrogen peroxide as enzyme substrate (Merck, 3% v/v) and leukodye (Fluka-3,3,5,5-tetramethylbenzidine, 0.1 g/l) was added and incubated in the dark for 30 min at 37°C. The enzyme-induced colour reaction was then stopped by adding 25 μl of H_2SO_4 2 M to the substrate solutions and finally the absorbance at 450 nm was determined spectrophotometrically (Perkin-Elmer Lambda 16). A quantitative relationship between the absorbance and the amount of protein(s) absorbed was determined from the PS latex depletion experiments [46].

2.5.2. Factor XII assay

The evaluation of the influence of the addition of VP–DMAm to BS to form T-IPNs on blood coagulation was made according to the method of interaction between the test materials and coagulation factor XII (FXII). The FXII activation measurements were performed by chromogenic peptide substrate assay with the tetrapeptide Bz–lle–Glu–Gly–Arg *p*-nitrophenylanilide (S-2222) [47–49]. Thus, BS/VP–DMAm and BS films with a total surface area of 1 cm^2 were put into 0.2 ml of human plasma and incubated for 1 h at 0°C to prevent inactivation of the kallikrein by the inhibitors in plasma. A chromogenic peptide substrate solution (Sigma, S-2302) of volume 300 μl was added to 300 μl of dilute human plasma control and incubated for 10 min at 37°C. After the addition of 300 μl of acetic acid to stop the reaction, the absorbance of the reacted chromogenic substrate was measured spectrophotometrically at 405 nm.

2.5.3. Kinetics of thrombus formation

The kinetics of thrombus formation onto polymeric surfaces was detailed previously [50,51]. Thus, whole human blood was added to one part of acid–citrate–dextrose (ACD) for nine parts of blood. The resultant ACD blood was placed on a glass plate, BS and BS/VP–DMAm T-IPNs. Clotting was initiated by adding aqueous $CaCl_2$ solution, and the weight of thrombus formed during 12 min was weighed. The relative weights of thrombus formed on different samples were determined, with that formed on a glass plate being taken as 100%.

2.5.4. Platelet adhesion to polymer surfaces

The platelet adhesion onto BS and BS/VP–DMAm T-IPNs films was evaluated by using the methodology by Park et al. [52]. Thus, fresh samples of platelet-rich plasma (PRP) were prepared by collecting human blood into plastic syringes containing 3.8% sodium citrate solution (final dilution 1:9) to prevent blood coagulation. Blood was centrifuged at 200 *g* for 10 min at 4°C and the PRP supernatant was collected. The platelets were further centrifuged at 155 *g* for 20 min at 4°C and the PPP supernatant was mixed with the PRP to give a PRP with a final platelet concentration of 7×10^5 per microliter. The BS and BS/VP–DMAm T-IPNs films were put in appropriate Teflon tubes (0.5 ml) and equilibrated with 2 ml PBS buffer (pH 7.4, ionic strength = 0.01 M) at 37°C overnight. Prior to adhesion studies, the buffer was removed from the tubes and PRP (0.5 ml) was introduced into the Teflon tubes and incubated at 37°C for 1 h. A control sample of PRP incubated without the polymeric films was used as a reference. The platelets were counted by phase microscopy and the degree of platelet adhesion was determined by

$$\%\,\text{Adhesion} = (C_{p0} - C_{pt})/C_{p0},$$

where C_{p0} and C_{pt} are the counts of the number of platelets before and after contact with BS and BS/VP–DMAm T-IPNs films, respectively.

3. Results and discussion

The solubility parameter (δ) of Biospan™ has a value of 10.5 ($cal^{1/2}/cm^{3/2}$) [53], and the VP–DMAm copolymers a value between 10.2 ($cal^{1/2}/cm^{3/2}$) (PVP) and 10.7 ($cal^{1/2}/cm^{3/2}$) (PDMAm), calculated in this work using the additive groups contribution method of Van Krevelen [54]. Considering that the solubility parameters of the two components differ by only 0.20–0.30 ($cal^{1/2}/cm^{3/2}$) , the application of the Krause method of miscibility prediction shows that the system would be miscible at all compositions [55].

All of the prepared BS/VP–DMAm T-IPNs remained transparent, suggesting that macrophase separation does not occur, showing that the morphology of BS/VP–DMAm T-IPNs is closely related to the compatibility of two components.

Optical microscopy was used to study the effect of the VP content on VP–DMAm copolymers added to BS on the phase separation of BS/VP–DMAm T-IPNs. In relation to BS films, no superstructures were observed by phase contrast microscopy with the addition of VP–DMam copolymers, suggesting that a miscible macromolecular interpenetration is obtained independent of the copolymer composition used.

Since the VP units exhibit fluorescent properties when excited with light of wavelength 290 nm, fluorescence spectroscopy was used to gain an understanding of the forces governing the solvation of the polymer networks on a molecular level of the BS/VP–DMAm systems. Thus, the change in the fluorescence emission of the VP present in the T-IPNs may be due to the formation of a twisted intramolecular charge transfer state induced by changes in free volume and/or micropolarity surrounding the VP–DMam copolymers [56].

Fig. 2 shows the normalised steady-state emission spectra of the T-IPNs systems as a function of VP content in VP–DMAm copolymers. Thus, the results plotted in Fig. 2 show that the intensities of the emission at the λ_{em} wavelength of the lactam units increase with their content in the VP–DMAm copolymer present in T-IPNs systems.

The fluorescence emission spectra were deconvoluted and the area ratios of the emission peaks relative to the BS were determined. The results are shown in Fig. 3 and indicate an increment, corresponding to a decreasing energy transfer as the VP content in the copolymer is increased but levels off to a constant value for T-IPNs systems in which the BS/VP–DMAm T-IPNs contain 60% of the lactam units.

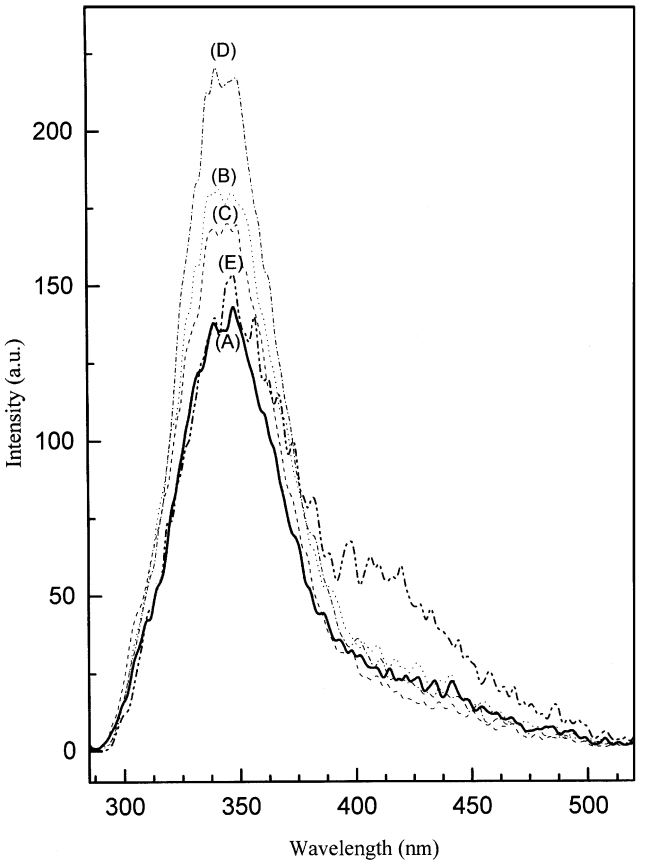

Fig. 2. Fluorescence spectra of the BS/VP–DMAm T-IPNs as a function of VP compositions (in copolymers): (A) BS; (B) VP100BS; (C) VP8BS; (D) VP29BS; (E) VP63BS.

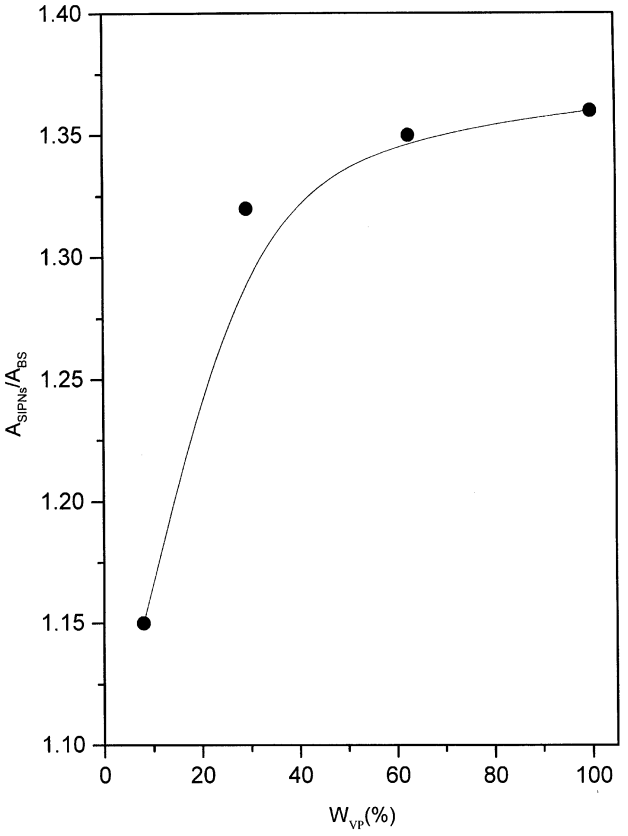

Fig. 3. Change of normalised area ratios from fluorescence spectra as a function of VP content in the copolymer for BS/VP–DMAm T-IPNs.

In T-IPNs systems containing a mixture of two polymers with donor–acceptor characteristics, energy transfer would be expected to be favoured if two polymeric species can freely interpenetrate one another in a single phase. If the systems separate into two phases, energy transfer will only occur in the neighbourhood of the phase boundary and consequently, the ratio of the emission intensities at λ_{em} increases. Thus, Fig. 3 may reflect the decreasing compatibility of the BS and VP–DMAm at high VP content in copolymer, leading eventually to a two-phase system. However, it was expected that incompatibility between BS and VP–DMAm at high VP content in the copolymer would be observed by optical microscopy. This was not observed. Thus, the plateau region in Fig. 3 observed at high VP content may reflect a smaller interfacial energy leading to an increased interfacial area due to rearrangements of the soft and hard segments of BS [57].

Fig. 4 shows ATR-FTIR spectra of pure BS and BS/VP–DMAm T-IPNs at room temperature in the carbonyl and ether stretching regions. It may be noted that with increasing VP content in the BS/VP–DMAm T-IPNs a decrease of the carbonyl band intensity at 1733 cm^{-1} together with an increasing of the ether band at 1112 cm^{-1} (corresponding to the polyether segment of BS) were detected. The new bands in the carbonyl (>C=O) region (1700–1734 cm^{-1}) and an increase in the intensities of the ether stretching bands (C–O–C) (1112 cm^{-1}) observed on the ATR-FTIR spectra for BS/VP–DMAm T-IPNs (Fig. 4) give some evidence that there may exist hydrogen bonds formed between the segmented polyurethane (BS) and the VP–DMAm copolymer.

Fig. 5 shows that the intensity ratio between the carbonyl regions of the BS/VP–DMAm T-IPNs and BS matrix increases with the increase in VP content. The intensity ratio of the ether stretching of the BS/VP–DMAm relative to BS decreased with the increment of the VP content in VP–DMAm copolymer added to BS. The magnitude of the intensity ratios of the carbonyl or ether relative to the BS matrix may correspond to the relative concentration of the hard and soft segments on the BS or BS/VP–DMAm surfaces. Thus, these results indicate that the addition of VP–DMAm copolymers with higher VP contents to BS matrix causes a surface enrichment of the lower surface free energy component (possibly, the polyether soft segment) in order to minimise the overall surface free energy of the binary macromolecular system [58,59].

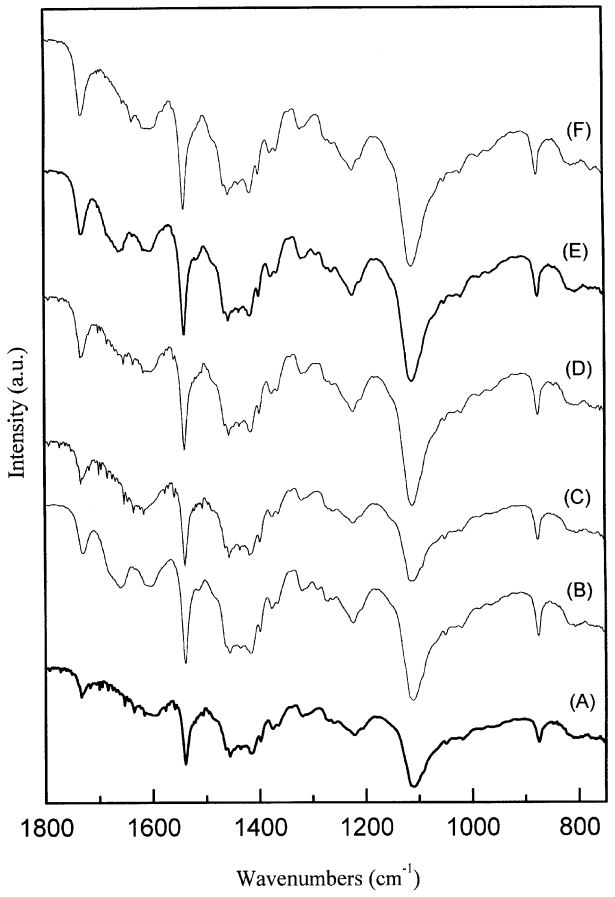

Fig. 4. ATR-FTIR spectra of (A) BS; (B) VP100BS; (C) VP63BS; (D) VP29BS; (E) VP8BS and (F) PDMAm.

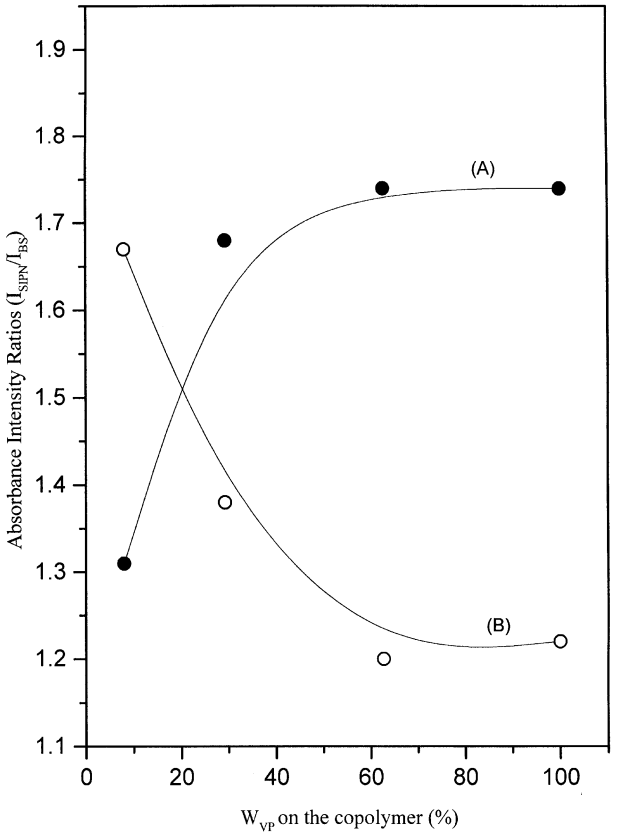

Fig. 5. Changes of STR-FTIR intensities with the VP content in the BS/VP–DMAm T-IPNs: (A) > C=O and (B) C–O–C.

Water plays an important role in determining the biocompatibility characteristic of the synthetic materials. The potential advantage of high water levels within the surface of the biomaterial in respect of the equivalence with normal tissues and especially for providing a low interfacial tension with blood, which would reduce protein adsorption and cell adhesion or activation has been recognised as an essential requisite for the utilisation of synthetic materials in contact with physiological fluids such as blood. Thus, the swelling behaviour of the BS/VP–DMAm T-IPNs should be expected to play an important role in the biocompatibility of these synthetic materials.

The VP–DMAm entangled in the BS matrix after exposure to an aqueous solution will swell. The swelling of the VP–DMAm exposed chains will exert some pulling force on the anchored segment, which adds to the force generated by the tendency of the water-soluble copolymer (VP–DMAm) to migrate into the aqueous phase and dissolve into the aqueous solution.

Thus, the permanence of the entangled VP–DMAm on the BS matrix depends on the ability of the solvated/embedded VP–DMAm chains to resist the pull force from the exposed swollen segments.

As is evident from Fig. 6, the level of water uptake increases with the content of vinylpyrrolidone units on the BS/VP–DMAm T-IPNs. It may be noted from Fig. 6 that the water sorption is mainly dominated by a Langmuir mode given an exothermic contribution to the sorption process, that is, the amount of water sorption decreases with increasing temperature.

The mechanism of water transport in the BS/VP-co-DMAm T-IPNs may be described by the following semi-empirical equation derived by Peppas [60,61]:

$$\frac{M_t}{M_\infty} = kt^n, \tag{1}$$

where n is an integration coefficient.

In case I or Fickian transport, where the rate of diffusion is much less than the rate of relaxation, $n = 0.5$; in case II transport, where diffusion is very rapid compared to rate of relaxation, $n = 1$. Non-Fickian systems lie between cases I and II, and n takes an intermediate value between 0.5 and 1.

Table 2 shows the n values for water sorption of BS/VP–DMAm T-IPNs swelling in PBS at 37°C. In general, the results indicate Fickian behaviour with

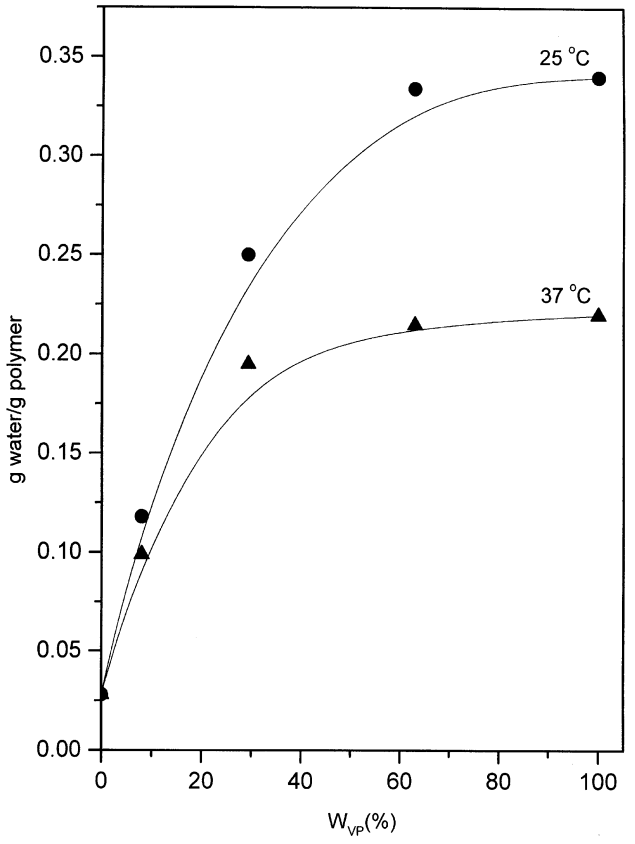

Fig. 6. Water uptake per dry polymer weight (g/g) for BS/VP–DMAm T-IPNs.

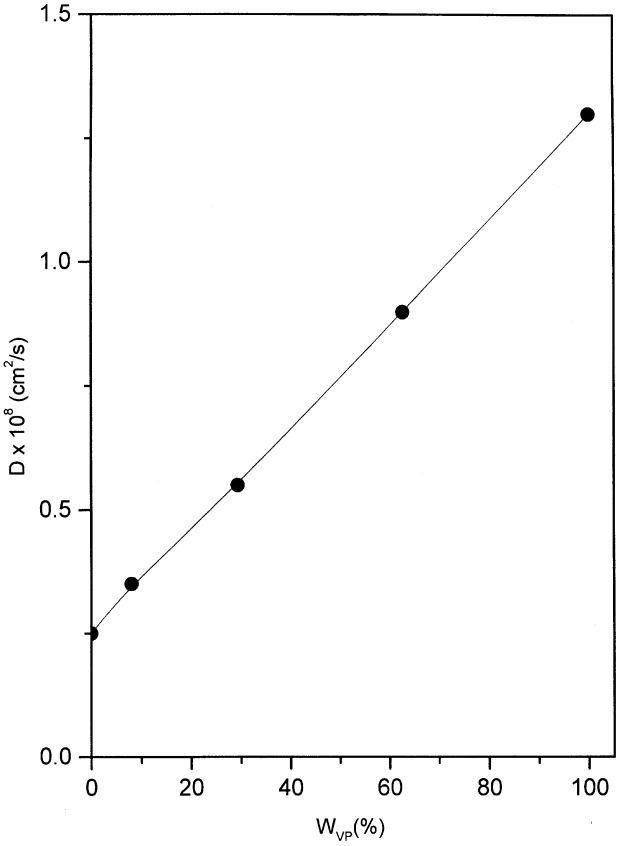

Fig. 7. Effect of VP content on water diffusion (PBS, pH 7.4, 37°C) of BS/VP–DMAm T-IPNs.

Table 2
Water sorption data *n* value of BS/VP–DMAm T-IPNs at 37°C in PBS

Sample	*n*
BS	0.36 ± 0.14
VP8BS	0.37 ± 0.10
VP29BS	0.41 ± 0.03
VP63BS	0.55 ± 0.12
VP100BS	0.48 ± 0.10

values of n ranging from 0.36 to 0.55 with confidence limits between 0.03 and 0.14. These results are an indication that chain relaxation is not as important as the phenomenon of penetrant transport in the swelling/deswelling process.

If the initial concentration, C_0, of the diffusant is constant at the surface and reaches a value C_{max} at equilibrium, then the solution of Eq. (1) gives [62]

$$\frac{M_t}{M_\infty} = 1 - \frac{8}{\pi^2}\sum_{n=0}^{\infty}\frac{1}{(2n+1)^2}\,e^{((-D(2n+1)^2\pi^2/h^2)t)}, \quad (2)$$

where M_t is the mass sorbed at time t, M_∞ is the mass sorbed at equilibrium time and h is the initial thickness of the polymer film.

The mass M, of diffusant taken up by the polymer as a function of time, is obtained by integrating Eq. (2) over the entire thickness, h, for obtaining

$$\ln\left(1 - \frac{M_t}{M_\infty}\right) = \ln\left(\frac{8}{\pi^2}\right) - \frac{D\pi^2 t}{h^2}, \quad (3)$$

where D represents the diffusion coefficient.

According to Eq. (3), the plot of $\ln(1 - M_t/M_\infty)$ vs. t should be linear at long diffusion times, and slopes of these lines are proportional to diffusion coefficients. As shown in Fig. 7, the water diffusion coefficients increased with increasing the lactam content on the T-IPNs films, indicating a greater motional freedom of the water molecules in the T-IPNs compared to the BS films.

However, at a weight fraction of water of 0.235 (at swelling equilibrium), the highest water content attained at swelling equilibrium, the diffusion coefficient is equal to 1.8×10^{-8} cm^2/s, which clearly indicates that the water molecules still possess a high degree of translational mobility and are not "tightly bound" or immobilised in the T-IPNs structure. A simple calculation using the Einstein equation for simple diffusion [63]

$$x = (2Dt)^{1/2} \quad (4)$$

illustrates that it would take only 0.28 s for a water molecule to diffuse a macroscopic distance of 1 mm at the lowest water content studied, indicating that the water molecules are indeed quite mobile. Thus, it is important to note that the diffusion coefficients of water at the highest composition of VP in BS/VP–DMAm T-IPNs are more than one order of magnitude less than that expected for the free diffusion of bulk water [64]. Thus, water molecules in the absorbed state are somewhat restricted by the T-IPNs structure, even at higher water contents.

No appreciable hysteresis in T-IPNs swollen/deswollen experiments (results not shown) was observed indicating that the water sorption by BS/DMAm is reversible and the systems remain homogeneous without significant migration of the VP–DMAm towards the BS surface to aqueous solution when compared with the total amount of VP–DMAm in the formulation.

The activation energy, E_D, for the process of diffusion is estimated from the Arrhenius relation [65,66]

$$D = D_0 e^{-E_D/RT}, \quad (5)$$

where D_0 is the pre-exponential factor, R the molar gas constant, T the absolute temperature and E_D the activation energy required to produce an opening between polymer chains segments large enough to allow the water to diffuse. The range of temperatures used was 298–310 K and the number of points in each curve was three (298, 303 and 310 K). There is a linear increase in the E_D values with the increasing of VP on the VP–DMAm copolymers added to BS as can be seen in Fig. 8.

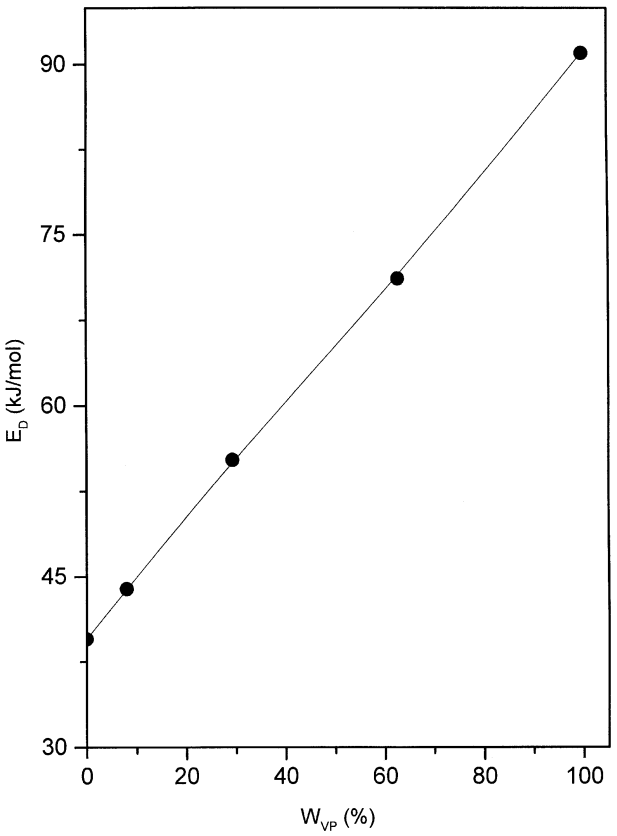

Fig. 8. Diffusion energy (E_D) of BS/VP–DMAm T-IPNs as a function of VP composition.

These results could be explained on the basis of Eyring's hole theory according to which the energy required "to open a hole" in the polymer matrix to accommodate a diffusing molecule bears a direct relationship with E_D [67]. Thus, the higher E_D values with the increase of VP in the VP–DMAm copolymer present in the T-IPNs may be interpreted in terms of the difficulty associated with the movement of the aggregates of water molecules through the polymer matrix. This difficulty may be associated with both intra- and interchain forces between the VP–DMAm copolymer and BS that must be overcome in order to create space for a unit diffusional jump of the water molecules.

The effect of the VP content on the diffusion or permeability of water in the BS/VP–DMAm T-IPNs is complex. Often the free volume of the hydrophilic polymer is lower than that of the hydrophobic polymer (BS) which tends to reduce the diffusion coefficient. However, at high activity of water, the plasticising effect can reverse this trend. As a result, there is no universal rule for how water permeability is affected by an increase in the VP content in the BS/VP–DMAm T-IPNs; but at high water activity, the permeability is generally increased by adding the hydrophilic VP–DMAm copolymers.

The surface free energy of a material should be able to provide the interaction energy required for protein or cell adhesion [68–70]. Thus, the surface of the materials must be characterised and controlled for the purpose of good biocompatibility. Especially, the surface characteristics of biomedical materials in water are important because they are generally used in wet state or aqueous solution.

The surface free energy components of the copolymers containing various weight fractions of VP units were calculated from the contact angle data of various liquids by using the Van Oss–Good methodology [71–73].

Fig. 9 shows the variation in the total water-equilibrated solid surface tension (γ_{SV}), and the solid–water interfacial tension (γ_{Sw}), as a function of the VP–DMAm composition added to BS to form T-IPNs. Thus, the solid–water interfacial tension, γ_{SV}, was seen to increase to near the value of the surface tension of pure water that is 72.1 dynes/cm when only PVP (VP100BS) was added to BS to form T-IPNs. If the T-IPNs surface were entirely covered with an adsorbed layer of water, then the interface would essentially consist of the adsorbed water layer in contact with the bulk water. In this case, γ_{Sw} would be expected to be near zero if the energies of adsorbed water and bulk water are similar. As can be seen in Fig. 9, starting from pure BS, γ_{Sw} decreased gradually to very near zero as pure PVP was added to the BS matrix.

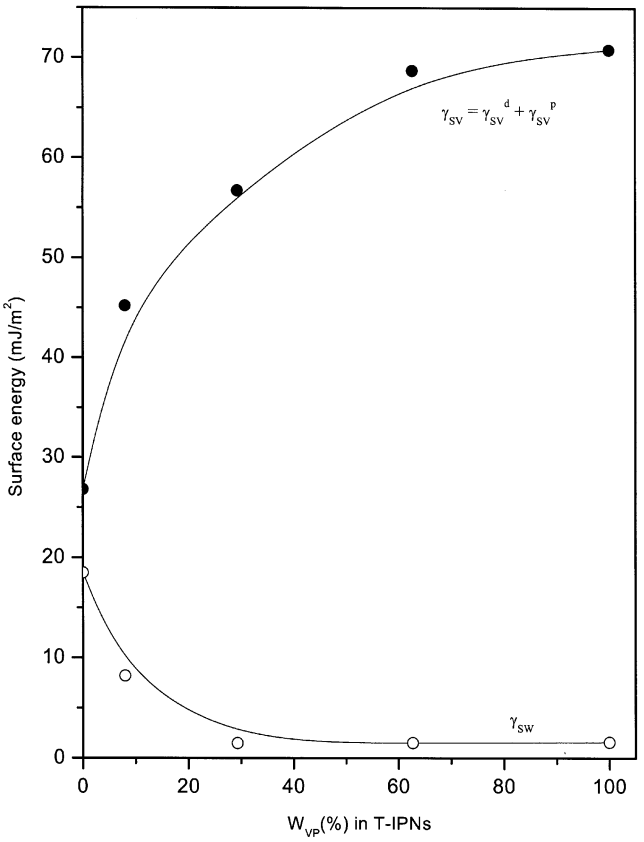

Fig. 9. Total water-equilibrated solid surface tension of BS and BS/VP–DMAm T-IPNs.

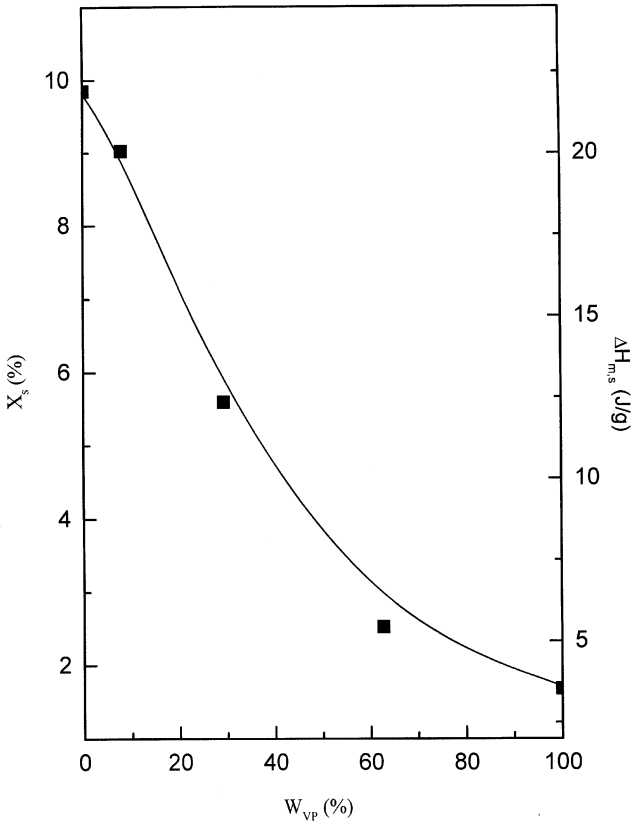

Fig. 10. Dependence of crystallinity (X_c) and heat of fusion ($\Delta H_{m,s}$) of the soft segment on BS with VP content on T-IPNs.

Table 3
Thermal properties determined by DSC[a]

Sample	W_{pvp} (%)	$T_{g,s}$ (°C)	$\Delta H_{c,s}$ (J/g)	$\Delta H_{m,s}$ (J/g)	X_s (%)
BS	—	−76.0	19.6	21.3	9.8
VP8BS	8.0	−79.5	18.1	20.0	9.0
VP29BS	29.3	−81.1	10.3	12.4	5.7
VP63BS	62.7	−81.8	4.0	5.6	2.5
VP100BS	100.0	−83.0	2.7	3.6	1.7

[a] W_{pvp} (%), $T_{g,s}$, $T_{m,s}$, $\Delta H_{c,s}$, $\Delta H_{m,s}$, and X_s are the weight percent of VP in the copolymer, glass transition temperature, melting temperature, heat of crystallisation, heat of fusion and percentage of crystallinity of soft segment, respectively.

Differential scanning calorimetry was utilised to examine whether the second-order transitions were affected by addition of the VP–DMAm copolymers in BS matrix. The DSC results are summarised in Table 3. The thermogram for pure BS showed the glass transition temperature of soft segments ($T_{g,s}$) of PTMO at −76°C, an exothermic peak at −26°C due to the crystallisation of PTMO phase, and a melting peak at 9°C characteristic of this crystalline phase.

The percent of crystallinity of soft-segment phase of BS (X_s) was determined by assuming a heat of fusion ($\Delta H_{m,s}$) equal to 221.6 (J/g) for 100% crystallinity of PTMO-2000 homopolymer and normalising the heat of fusion to unit weight of soft segment [74].

The glass transition temperature of hard domains ($T_{g,h}$) was found to be hardly discernible at 130°C and an endotherm at 280°C was attributed to the melting of hard segments. The thermal degradation of the BS occurred immediately after the melting of this point making it impossible to determine the heat of fusion of hard domains.

As shown in Fig. 10, both the percent of crystallisation and the heat of fusion of the soft-segment domains decreased with the increase of the VP amount in the T-IPNs. This fact indicates that the presence of a bulky bearing group such as pyrrolidone prevents the PTMO crystallisation.

The decrease of $T_{g,s}$ of the T-IPNs series with the increase of VP, as seen in Fig. 11, could be attributed to the greatest homogeneous or phase separation between the hard and soft segments, indicating the level of molecular mixing and adhesion at phase boundaries because of Biospan/VP–DMAm interpenetration and the formation of different domain sizes. In the case of VP8BS and

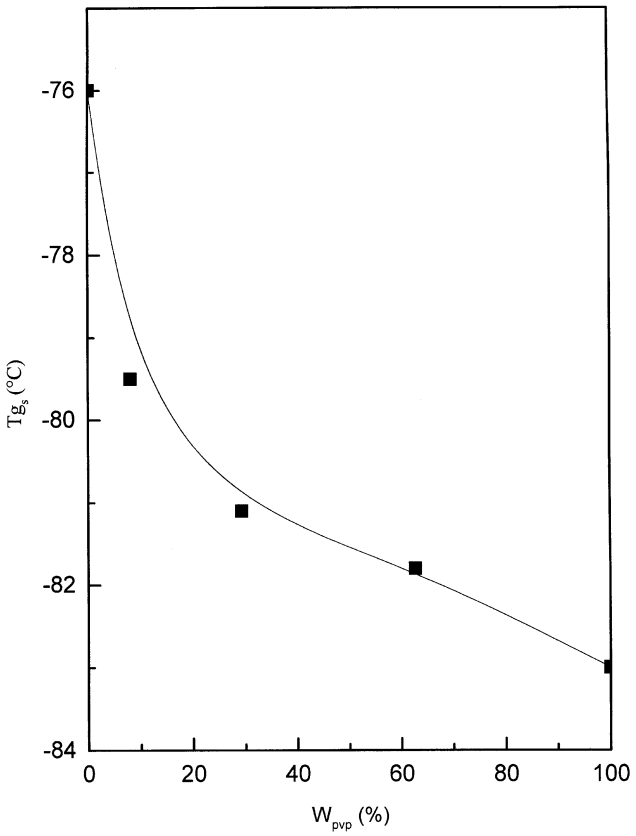

Fig. 11. Changes in glass transition temperatures of the BS soft segments ($T_{g,s}$) with VP content in BS/VP–DMAm T-IPNs.

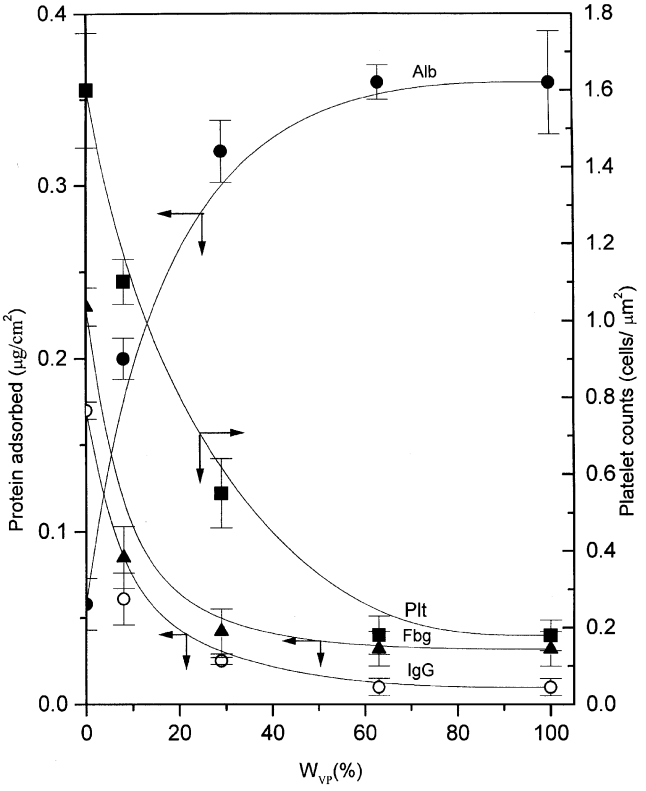

Fig. 12. VP content dependence of protein adsorption (Alb, Fbg, IgG) and adherent platelet numbers (Plt) onto BS/VP–DMAm T-IPNs.

VP29BS samples, the $T_{m,s}$ remained at the same value as pure BS (9°C), but in VP100BS and VP63BS T-IPNs only a small endothermic event at −11°C was observed.

The $T_{g,h}$ as well as $T_{m,h}$ values of the T-IPNs series did not show significant variation with respect to the pure BS. Thus, the incorporation of the VP–DMAm does not affect the hard-segment domains, due to the high concentration of urea groups whose hydrogen-bonding network enhances intradomain cohesion.

Intrinsic biological responses in the vascular systems may occur upon exposure to synthetic polymers. Such responses include protein adsorption, cell adhesion and activation and consequently blood coagulation.

Materials in contact with physiological fluids such as blood are exposed to a mixture of protein adsorbates that dominates the available surface area as dynamically forming surface layer, activated or passivated by the underlying synthetic surface.

The concentration of the adsorbate as well as the conformation of the constituent proteins will determine the adsorption and activation of subsequently interacting proteins and platelets.

The effect of protein adsorption on the antithrombogenicity of the synthetic materials has been investigated by many researchers [75–79]. It is well known that if the polymer material is considered to have a microphase-separated structure composed of a diffuse layer or hydrophilic and hydrophobic microdomains, the albumin (Alb), fibrinogen (Fbg) and γ-globulins (IgG), proteins of the plasma blood, are selectively adsorbed in the regions described above [80]. Thus, the knowledge of protein adsorption on foreign surfaces can improve the antithrombogenicity of materials used for blood-contacting devices.

The protein adsorption measurements of Alb, Fbg and IgG as well as platelet adhesion onto BS/VP–DMAm T-IPNs films are represented in Fig. 12. A possible mechanism that explained the properties of the obtained BS/VP–DMAm T-IPNs to prevent the Fbg and IgG adsorptions is based on a combination of the steric stabilisation effect and the particular molecular conformation in the aqueous solution. The steric repulsion resulting from osmotic pressure and elastic restoring forces competing with the van der Waals attraction between the BS/VP–DMAm T-IPNs and Fbg and IgG may be a determinant in the protein-adsorption process.

It is well known that after the adsorption of proteins onto the polymeric surface, the next event is the adhesion of platelets (blood cell) [81,82]. Thus, platelet adhesion is inhibited by prior adsorption of albumin and promoted

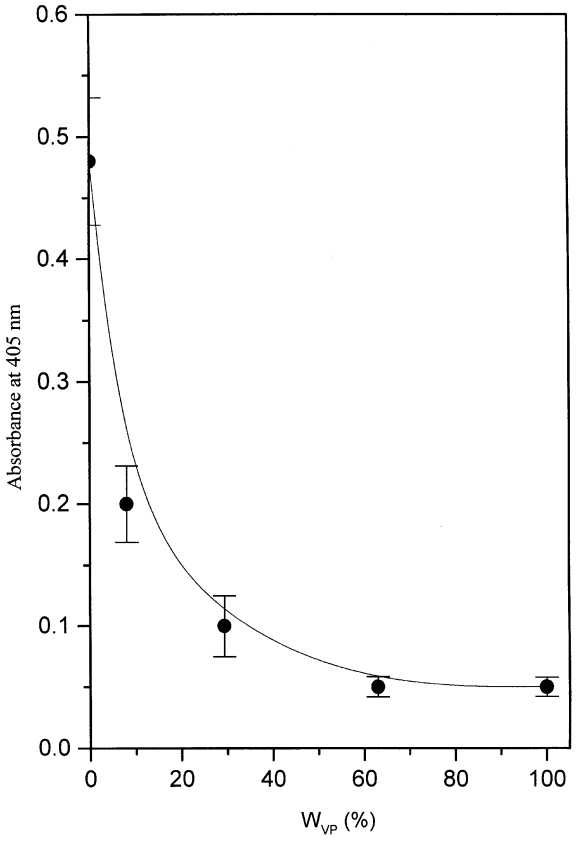

Fig. 13. Kallikrein activity induced by human plasma on BS/VP–DMAm T-IPNs.

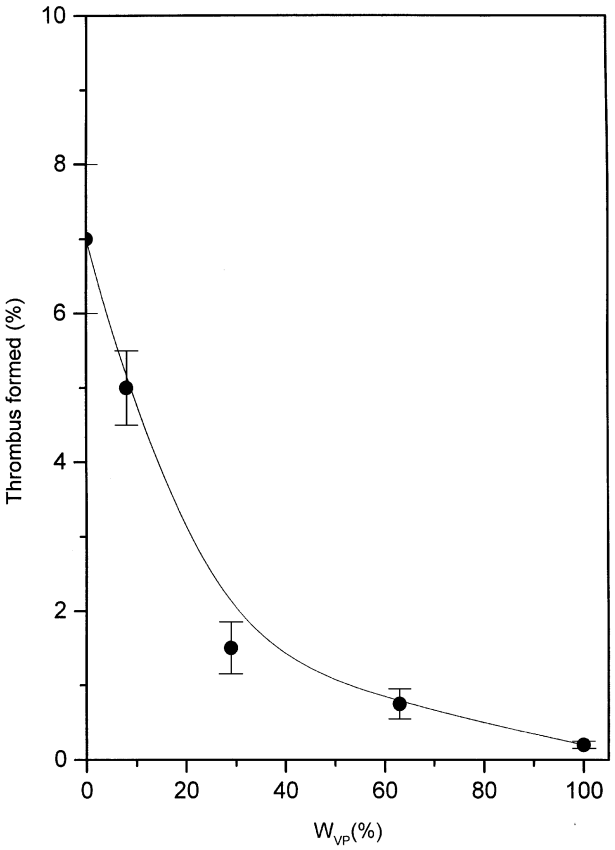

Fig. 14. Thrombus formation on BS/VP–DMAm T-IPNs of different VP compositions (reference: glass, 100% of thrombus formed).

when IgG or fibrinogen is preferentially adsorbed to synthetic surfaces [83,84].

Relationships between platelet adhesion and VP contents on the BS/VP–DMAm T-IPNs surfaces are shown in Fig. 12. The T-IPNs containing the VP–DMAm copolymers with higher VP contents show significant effects on the platelet adhesion.

The platelet adhesion for BS/VP–DMAm T-IPNS surfaces decreased with increasing amounts of VP on the VP–DMAm copolymer and therefore, they have better blood compatibility than BS surfaces.

The protein composition of the adsorbed monolayer onto the polymer surface may activate the platelets, which then adhere and aggregate to one another through membrane glycoprotein complexes, leading to thrombus formation [85].

The contact phase between blood and a polymeric surface comprises a large complex number of reactions which take place during the first time of initial blood contact and overlap with protein adsorption or displacement and boundary layer development [86,87].

In biomaterials, factor XII is central to the reactions of the blood contact phase. A recent review on the theoretical understanding of the events which take place during the interaction of biomaterials with blood and the importance of factor XII as a blood contact phase has been reported by Basmadjian et al. [88].

Factor XII activation induces a series of intrinsic coagulation system chain reactions that are capable of triggering coagulation in the presence of a surface. Thus, in this study, the amount of activated factor XII was evaluated from the kallikrein produced. Fig. 13 indicates the kallikrein activity induced by interaction between human plasma and BS/VP–DMAm T-IPNs. Less kallikrein was observed on the BS/VP–DMAm T-IPNs films than on the non-modified BS films indicating that intrinsic coagulation factor XII is less active on the segmented polyurethane containing the hydrophilic VP–DMAm copolymers with higher VP contents.

The dependence of thrombus formation on the VP content of the VP–DMAm added to BS matrix is demonstrated in Fig. 14, which is very similar to the dependence of platelet adhesion and fibrinogen or γ-globulin adsorption on the VP composition of the BS/VP–DMAm T-IPNs. It was also found that thrombus formation is suppressed with increasing VP content in the VP–DMAm copolymers added to BS to form T-IPNs.

4. Conclusions

In theory, the best way to immobilise hydrophilic polymers permanently onto a surface is by covalent bonding processes, but such methods are generally difficult and too costly for commercialisation. One alternative involves the preparation of interpenetrating polymer networks. This technique is much easier and more economical than covalent bonding.

In principle, such systems offer a simple and attractive way of continuously controlling the interaction with water and thus, a way to tailor water and proteins adsorption, cell adhesion and consequently the blood compatibility of the material.

In this work it is demonstrated that the VP content on BS/VP–DMAm T-IPNs is an important factor for the adsorption processes of plasma proteins such as albumin, γ-globulin and fibrinogen.

The decreasing of fibrinogen and γ-globulin adsorption and increased adsorption of albumin for T-IPNs containing VP–DMAm copolymers with increased VP content as well as the existence of a better hemocompatibility hint that it must be due to the surface composition, molecular mobility of the BS and VP–DMAm chains and interaction of the plasma proteins with water in the BS/VP–DMAm T-IPNs surfaces. However, a more detailed investigation is necessary to make clear the influence of the bulk structure and their relation with the blood compatibility of the BS/VP–DMAm T-IPNs surfaces obtained in this work. Additional and more comprehensive studies are being carried out in order to speculate upon the non-thrombogenic character of the BS/VP–DMAm T-IPNs systems and the results will be reported elsewhere.

Acknowledgements

G. Abraham thanks National Research Council (CONICET) of Argentina for the fellowship awarded. A.A.A. de Queiroz is grateful to the MEC/CSIC which provided the opportunity for his stay in Spain and wishes also to thank Professor Roberto R. Ribeiro and Professor Osvair L. de Castro of Clinical Analyses Laboratory of the Camilo Castelo Branco University/Faculty of Pharmaceutical Sciences (CAL/UCCB, SP/Brazil) for their technical assistance with respect to the biological assays.

References

[1] Borgdorff P, Kok WEM, Van den Bos GC. Extracorporeal circuits and autoregulation: effect of albumin coating. Am J Physiol 1992;263:H1397–401.

[2] Solomon DD, Sheretz RJ. Antibiotic releasing polymers. J Controlled Release 1987;6:343–52.

[3] San Roman J, Bujan J, Bellon JM, Gallardo A, Escudero MC, Jorge E, de Haro J, Alvarez L, Castillo-Olivares JL. Experimental study of the antithrombogenic behavior of dacron Vascular grafts coated with hydrophilic acrylic copolymers bearing salicylic acid residues. J Biomed Mater Res 1996;32(1):19–27.

[4] Mochizuki A, Seita Y, Nakashima T, Endo F, Yamashita S. Polyether-segmented nylon hemodialysis membranes. V. Evaluation of blood compatibility of polyether-segmented nylons. J Appl Polym Sci 1998;67(7):1253–7.

[5] Faxon DP. Practical angioplasty. Raven Press: New York, 1993 [chapter 2].

[6] Anderson AB, Clapper DL. Coatings for blood-contacting devices. Med Plast Biomater 1998;Mar:30–48.

[7] Mathur AB, Collier TO, Kao WJ, Wiggins M, Schubert MA, Hiltner A, Anderson JM. In vivo biocompatibility and biostability of modified polyurethanes. J Biomed Mater Res 1997; 36:246–57.

[8] Helmus MN, Tweden K. Materials selection. In: Wise DL, Trantolo DJ, Altobelli DE, Yaszemski MI, Gresser JD, Schwartz ER, editors. Encyclopedic handbook of biomaterials and bioengineering, vol. 1. New York: Marcel Dekker, 1995. p. 27–59.

[9] Coury AJ, Cobinan KE, Cahalan PT, Jevne AH. Biomedical uses of polyurethanes. In: Frisch KC, Klempner D, editors. Advances in urethane science and technology. Lancaster, PA: Technomic, 1984. p. 130–68.

[10] Lelah MD, Cooper SL. Polyurethanes in medicine. Boca Raton, FL: CRC Press, 1986.

[11] Li YJ, Nakamura N, Wang YF, Kodama M, Nakaya T. Synthesis and haemocompatibilities of new segmented polyurethanes and poly(urethane urea)s with poly(butadiene) and phosphatidyl choline analogs in the main chains and long-chain alkyl groups in the side chains. Chem Mater 1997;9(7):1570–7.

[12] Abraham GA, Frontini PM, Cuadrado TR. Physical and mechanical behavior of sterilized biomedical segmented polyurethanes. J Appl Polym Sci 1997;65(6):1193–203.

[13] Savelyev YV, Akhranovich ER, Grekov AP, Privalko EG, Korskanov VV, Shtompel VI, Privalko VP, Pissis P, Kanapitsas A. Influence of chain extenders and chain end groups on properties of segmented polyurethanes. I. Phase morphology. Polymer 1998;39(15):3425–9.

[14] Pissis P, Kanapitsas A, Savelyev YV, Akhramovich ER, Privalko EG, Privalko VP. Influence of chain extenders and chain end groups on properties of segmented polyurethanes. II. Dielectric study. Polymer 1998;39(15):3431–5.

[15] Suh SW, Kim WG, Kim HC, Min BG. A new polymer valve for mechanical circulatory support systems. Int J Artif Organs 1996;19(12):712–8.

[16] Liotta D, Alvarez CB. Chronic heart assist system. In: Unger F, editor. Assisted circulation IV. Berlin: Springer, 1994.

[17] Liotta D. Conicet — Procoar investigators. Direct linear-pull skeletal muscle-powered for chronic implantable assist blood pump for end-stage heart failure (CHF). Fifth International Symposium on Cardiac Surgery, Rome, Italy, May 1993.

[18] Yoda R. Elastomers for biomedical applications. J Biomater Sci Polymer Edn 1998;9(6):561–626.

[19] Shimada M, Miyara M, Tahara H, Shinohara I, Okano T, Kataoka K, Sakurai Y. Synthesis of 2-hydroxyethyl methacrylate-dimethylsiloxane block copolymers and their ability to suppress blood platelet aggregation. Polym J 1983; 15(9):649–56.

[20] Ikada Y. Blood-compatible polymers. Adv Polym Sci 1984; 57:104–38.

[21] de Queiroz AAA, Barrak ER, Castro SC. Thermodynamic analysis of the surface of biomaterials. J Mol Struct (Theochem) 1997;394:271–9.

[22] Williams DF. Fundamentals aspects of biocompatibility. Boca Raton, FL: CRC Press, 1990.

[23] Andrade JD. Surface and interfacial aspects of biomedical polymers. New York: Plenum Press, 1985.
[24] Okano T, Aoyagi T, Kataokak K, Abe K, Sakurai Y, Shimada M, Shinohara I. The hydrophilic-hydrophobic microdomain surface having the ability to supress platelet adhesion and their in vivo antithrombogenicity. J Biomed Mater Res 1986;20:919–25.
[25] Nair PD, Jayabalan M, Krishnamurthy VN. Polyurethane polyacrylamide IPNs. I. Synthesis and characterization. J Polym Sci Part A: Polym Chem 1990;28:3775–86.
[26] Jones DS, Bonner MC, Gorman SP, Akay M, Keane PF. Sequential polyurethane-poly(methylmethacrylate) interpenetrating polymer networks as ureteral biomaterials: mechanical properties and comparative resistance to urinary encrustation. J Mater Sci Mater Med 1997;8(11):713–7.
[27] Sperling LH. In: Klemper D, Sperling LH, Utracki LA, editors. Interpenetrating polymer networks. Washington: ACS, 1994. p. 5, 6 [Chapter 1].
[28] Ali SAM Hourston DJ. In: Klempner D, Frisch KC, editors. Adv. interpenetrating polymer networks. Lancaster, PA: Technomic, 1994. p. 17–43.
[29] Okano T, Nishiyama S, Shinohara I, Akaike T, Sakurai Y, Kataoka K, Tsuruta T. Effect of hydrophilic and hydrophobic microdomains on mode of interaction between block polymer and blood platelets. J Biomed Mater Res 1981;15:393–9.
[30] Okano T, Uruno M, Sugiyama N, Shimada M, Shinohara I, Katakaoka K, Sakurai Y. Suppression of platelet activity on microdomain surfaces of 2-hydroxyethylmethacrylate-polyether block copolymers. J Biomed Mater Res 1986;20:1035–42.
[31] Migliaresi C, Nicolais L, Giusti P. Chiellini E, editors. Polymers in medicine III. Amsterdam, Netherlands: Elsevier, 1988.
[32] Tomita N, Tamai S, Okajima E, Hirao Y, Ikeuchi K, Ikada Y. Biomaterials lubricated for minimum frictional resistence. J Appl Biomater 1994;5:175–81.
[33] de Queiroz AAA, Gallardo A, San Román J, Higa OZ. Hemocompatible properties of polymeric derivative of paracetamol. J Biomater Sci Polymer Edn 1995;7(6):523–30.
[34] de Queiroz AAA, Castro SC, Higa OZ. Adsorption of plasma proteins to DMAA hydrogels obtained by ionizing radiation and its relationship with blood compatibility. J Biomater Sci Polym Edn 1997;8(5):335–47.
[35] Vijayasekaran S, Chirila TV, Hong Y, Tahija SG, Dalton PD, Constable IJ, McAllister IL. Poly(1-vinyl-2-pyrrolidone) hydrogels as vitreous substitutes: histopathological evaluation in the animal eye. J Biomater Sci Polymer Edn 1996;7(8):685–96.
[36] Mark EJ, Okano T, Kim SW. Hydrogels in medicine and pharmacy. In: Peppas NA, editor. Boca Raton, FL: CRC Press, 1987.
[37] Forman MR, Helmus MN, Hostettler F, Ding N, Rhum D. Process for producing commingled polyurethane-urea and poly(*N*-vinylpyrrolidone) polymer hydrogel coatings. USA Patent 95–384711, 1 Feb 1995.
[38] Forman MR, Helmus MN, Hostettler F, Ding N, Rhum D. Hydrogel coatings containing a polyurethane-urea polymer hydrogel commingled with a poly(*N*-vinylpyrrolidone) polymer hydrogel. USA Patent 95–382318, 1 Feb 1995.
[39] Elton RK. Lubricious hydrogel protective coatings for plastic and rubber medical devices to be in contact with skin. Eur Pat Appl EP 483941 A2, 6 May 1992.
[40] de Queiroz AAA, Gallardo A, San Román J. Vinylpyrrolidone *N*,*N*′-dimethylacrylamide water-soluble copolymers: synthesis, physical-chemical properties and proteic interactions. Biomaterials 2000;21:1631–43.
[41] Bulai A, de Queiroz AAA, Gallardo A, San Román J. Microstructural analysis of *p*-acryloyloxy-acetanilide and *N*,*N*-dimethylacrylamide copolymers of biomedical interest by NMR. Polymer 1999;40:4953–60.
[42] Owens DK, Wendt RC. Estimation of the surface free energy of polymers. J Appl Polym Sci 1969;13:1741–7.
[43] Wu S. Polymer interface and adhesion. New York: Marcel Dekker, 1982.
[44] Breemhaar W, Brinkman E, Ellens DJ, Beugeling T, Bantjes A. Preferential adsorption of high density lipoprotein from blood plasma onto biomaterials surfaces. Biomaterials 1984;5:269–74.
[45] Van Damme H S, Beugeling T, Ratering MT, Feijen J. Protein adsorption from plasma onto poly(*n*-alkylmethacrylate) surfaces. J Biomater Sci Polym Edn 1991;3(1):69–84.
[46] Norde W, Lijklema J. The adsorption of human plasma albumin and bovine pancreas ribonuclease at negatively charged polystyrene surfaces. I. Adsorption isotherms. Effect of charge, ionic strength and temperature. J Colloid Interface Sci 1978;66:257–65.
[47] Gallimore MJ, Rees WA, Fuhrer G, Heller W. A direct chromogenic peptide substrate assay for Hageman factor (FXII). Fibrinolisis 1987;1(2):123–7.
[48] Hoem NO, Johannesen S, Briseid K. Assay of factor XII in human plasma using prekallikrein or the chromogenic peptide S-2222 as substrates — significance of the functional state of plasma kallikrein. Thromb Res 1989;54(3):197–205.
[49] Jones DW, Gallimore MJ, Winter M. An automated chromogenic peptide substrate assay for coagulation factor XII. Blood Coagulation Fibrinolysis 1998;9(2):183–7.
[50] de Queiroz AAA, Barrak ER, Gil HAC, Higa OZ. Surface studies of albumin immobilized onto PE and PVC films. J Biomater Sci Polymer Edn 1997;8(9):667–81.
[51] de Queiroz AAA, Castro SC, Higa OZ. Adsorption of plasma proteins to DMAA hydrogels obtained by ionizing radiation and its relationship with blood compatibility. J Biomater Sci polymer Edn 1997;8(5):335–47.
[52] Park KD, Okano T, Nojiri C, Kim SW. Heparin immobilization onto segmented polyurethaneurea surfaces, effect of hydrophilic spacers. J Biomed Mater Res 1988;22:977–92.
[53] Ryan AJ, Stanford JL, Still RH. Calculation of solubility parameters of typical structural units present in segmented polyurethanes, poly(urethane urea)s and polyureas formed by reaction injection moulding. Polym Commun 1988;29:196–8.
[54] Van Krevelen DW. Properties of polymers: correlations with chemical structure. Amsterdam: Elsevier, 1972.
[55] Krause S. Polymer blends. New York: Academic Press, 1970. p. 48–50.
[56] Fredrickson GH, Helfand E. Trap fluorescence experiments for the study of interfacial structure. Macromolecules 1986;19:2601–5.
[57] Williamson SL, Armentrout RS, Porter RS, McCormick CL. Microstructural examination of semi-interpenetrating networks of poly(*N*,*N*′-dimethylacrylamide) with cellulose or chitin synthesized in lithium chloride/*N*,*N*′-dimethylacrylamide. Macromolecules 1998;31:8134–41.
[58] Li YJ, Yokawa T, Matthews KH, Chen TM, Wang YF, Kodama M, Nakaya T. Synthesis and blood compatibility evaluation of segmented polyurethanes based on cholesterol and phosphatidylcholine analogous moieties. Biomaterials 1996;17:2179–89.
[59] Takahara A, Jo NJ, Kajiyama T. Surface molecular mobility and platelet reactivity of segmented poly(etherurethaneureas) with hydrophilic and hydrophobic soft segment components. J Biomater Sci Polym Edn 1989;1(1):17–29.
[60] Ritger PI, Peppas NA. A simple equation for description of solute release. I. Fickian and non Fickian release from non-swellable devices in the form of slabs, spheres, cylinders or discs. J Controlled Release 1987;5:23–6.
[61] Bell CL, Peppas NA. Water, solute and protein diffusion in physiologically responsive hydrogels of poly(methacrylic acid-*g*-ethylene glycol). Biomaterials 1996;17:1203–8.
[62] Vieth WR. Diffusion in and through polymers. Munich: Hansen, 1991.
[63] Assaf Y, Cohen Y. Non-mono-exponential attenuation of water and *N*-acetil aspartate signals due to diffusion in brain tissue. J Magn Res 1998;131(1):69–85.

[64] Lide DR. CRC handbook of chemistry and physics, 73rd ed. Boca Raton, FL: CRC Press, 1992–93.
[65] Rowland SP. Water in polymers. Washington: ACS, 1980.
[66] Arvanitoyannis I, Blanshard MV. Anionic copolymers of octanelactam with laurolactam (nylon 8/12 copolymers). VII. Study of diffusion and permeation of gases in undrawn and uniaxially drawn (conditioned at different relative humidities) polyamide films. J Appl Polym Sci 1993;47:1933–59.
[67] Ewalinski BJ, Eyring H, Reese CE. Diffusion and membrane permeability. J Phys Colloid Chem 1949;53:1426–51.
[68] Lu DR, Park K. Protein adsorption on polymer surfaces: calculation of adsorption energies. J Biomater Sci Polym Edn 1990;1(4):243–60.
[69] Schakenraad JM, Busscher HI, Wildevuur CRH, Arends J. The influence of substratum surface free energy on spreading of various cell-types on polymers. Adv Biomater 1986;6:263–8.
[70] Schakenraad JM, Arends J, Busscher HJ, Dijk F, Van Wachem PB, Wildevuur CRH. Kinetics of cell spreading on protein precoated substrata: a study of interfacial aspects. Biomaterials 1989;10(1):43–50.
[71] Janczuk B, Bialopiotrowicz T. The total surface free energy and the contact angle in the case of low energetic solids. J Colloid Interface Sci 1990;140(2):362–72.
[72] van Oss CJ, Good RJ. Surface tension and the solubility of polymers and biopolymers: The role of polar and apolar interfacial free energies. J Macromol Sci Chem 1989; A26:183–203.
[73] van Oss CJ, Chaudhury MK, Good RJ. Interfacial Lifshitz-van der Waals and polar interactions in macroscopic system. J Chem Rev 1988;88:927–41.
[74] Tanaka A, Vemura S, Ishida Y. Dielectric absorption of polyoxymethylene obtained from three crystalline cyclic formaldehyde oligomers by radiation-induced polymerization. J Polym Sci Polym Phys Edn 1972;10:2093–6.
[75] Mandenius CF, Ljunggren L. Ellipsometric studies of plasma protein adsorption on membrane polymers for blood purification. Biomaterials 1991;12(4):369–73.
[76] Leonard EF, Vroman L. Is the Vroman effect of importance in the interaction of blood with artificial materials? J Biomater Sci Polym Edn 1991;3(1):95–197.
[77] Williams DF. Fundamental aspects of biocompatibility. Boca Raton, FL: CRC Press, 1990.
[78] Andrade JD. Surface and interfacial aspects of biomedical polymers. New York: Plenum Press, 1985.
[79] Piskin E, Hoffman AS. Polymeric biomaterials. Netherlands: Martinus Nijhoff, 1986.
[80] Goodman SL, Simmons SR, Cooper SL, Albrecht RM. Preferential adsorption of plasma proteins onto apolar polyurethane microdomains. J Colloid Interface Sci 1990;139(2):561–70.
[81] Kroschwitz JI, editor. Polymers: biomaterials and medical applications. New York: Wiley, 1989.
[82] Hoffman AS. Applications of synthetic polymeric biomaterials in medicine and biotechnology. In: Martuscelli E, Marchetta C, Nicolais L, editors. Future trends in polymer science and technology. Lancaster: Technomic, 1987.
[83] Absolom DR, Zingg W, Policova Z, Neumann AW. Determination of surface tension of protein-coated materials by means of the advancing solidification front technique. Trans Am Soc Artif Org 1983;29:146–51.
[84] Meumer S, Heijnen HFG, Ijsseldijk MJW, Orlando E, de Groot PG, Sixma JJ. Platelet adhesion to fibronectin in flow: the importance of von Willebrand factor and glycoprotein Ib. Blood 1995;86:3452–60.
[85] Phillips DR, Charo IF, Parise LV, Fitzgerald LA. The platelet membrane glycoprotein IIb–IIIa complex. Blood 1988;71:831–43.
[86] Gregory K, Basmadjian D. An analysis of the contact phase of blood coagulation: Effects of shear rate and surface are intertwined. Ann Biomed Engng 1994;22:184–93.
[87] Courtney JM, Lamba NMK, Sundaram S, Forbes CD. Biomaterials for blood-contacting applications. Biomaterials 1994; 15(10):737–44.
[88] Basmadjian D, Sefton MV, Baldwin SA. Coagulation on biomaterials in flowing blood: some theoretical considerations. Biomaterials 1997;18:1511–22.